[CANCER RESEARCH 61, 8408–8411, December 1, 2001]

Advances in Brief

Computer Modeling Implicates Stem Cell Overproduction in Colon Cancer Initiation[1]

Bruce M. Boman,[2] Jeremy Z. Fields,[3] Oliver Bonham-Carter,[4] and Olaf A. Runquist

*Division of Genetic and Preventive Medicine, Thomas Jefferson University, Philadelphia, Pennsylvania 19107 [B. M. B.]; CA*TX, Inc., Gladwyne, Pennsylvania 19035 [J. Z. F., O. B-C.]; and Department of Chemistry, Hamline University, St. Paul, Minnesota 55104 [O. A. R.]*

Abstract

On the basis of our investigation of the premalignant crypt phenotype in familial adenomatous polyposis patients, the hypothesis is developed that tumor initiation in the colon is caused by crypt stem cell overproduction. A novel kinetic model for the colonic crypt was used to investigate how the earliest tissue abnormality (altered crypt labeling index) arises in these patients who have a mutant *APC* genotype. Only an increase in crypt stem cell number, not changes in the rate of cell cycle proliferation, differentiation, or apoptosis of the non-stem cell population, simulated this abnormality. This suggests that APC regulates the number of stem cells in the colonic crypt and when the cells become mutant, an expansion of the crypt stem cell population results.

Introduction

Mechanisms that cause normal tissues to become malignant involve an "enormously complex process" (1). Complexity in carcinogenesis occurs at many hierarchical levels including DNA, RNA, proteins, intracellular pathways, intercellular interactions, tissues, organs, individuals, families, society, and many others. At the DNA level, for example, tumor cells accumulate mutations in many genes. Because this complexity is compounded further by interactions among different levels, conventional *in vivo* and *in vitro* experiments have limitations in the study of cancer formation. As a result, little is known about how cancer-causing genetic mutations change the behavior of normal cells in a way that leads to alterations occurring at higher levels of complexity. Even in apparently simple situations, where an individual has a cancer-predisposing germ-line mutation, the cellular mechanism that links the mutation to neoplastic changes at the tissue level is unknown.

Because of this complexity of biological systems and the inherent limitations of biological experiments to resolve this dilemma, we used computer modeling. We modeled (Fig. 1) cellular mechanisms that might link a cancer-predisposing germ-line mutation to the earliest known tissue change in the development of CRC.[5] We chose to study FAP, because both the initiating genetic event (germ-line *APC* mutation) and earliest tissue change (proliferative shift) have been identified (2). Indeed, this tissue abnormality was first reported nearly 4 decades ago (3, 4). The proliferative shift involves an upward shift (toward the crypt top) in the distribution (LI) of DNA-synthesizing (S-phase) cells in histologically normal-appearing colonic crypts of FAP patients. The biological data sets of Potten *et al.* (5) for LI of control and FAP crypts (Fig. 2*A*) were used for our computer simulation. In this study, only histologically normal-appearing FAP crypts were analyzed (5), which excludes aberrant crypt foci.

Materials and Methods

Mechanisms to be Tested. Although the initiating genetic event (*APC* mutation) and the earliest tissue event (proliferative shift in histologically normal crypts) in CRC development are characterized in FAP, the cellular mechanism linking these events remains unknown. Four mechanisms have been suggested previously. Three invoke a change in the rate of cell cycle proliferation and/or differentiation as the cause of the abnormal crypt LI pattern. These include: (*a*) a loss of regulatory control that normally suppresses DNA synthesis during cell migration in the upper portions of the crypt (6); (*b*) a decrease in duration of the G_1 cell cycle phase (7); and (*c*) a decline in differentiation of epithelial cells in colonic crypts (8). A fourth invokes an abnormality in STs in the origin of CRC (9). Further reasoning for this last mechanism comes from an animal model of FAP. Moser *et al.* (10) found histological evidence of different cell lineages in intestinal adenomas and proposed that "tumorigenesis in $APC^{Min/+}$ mice may be initiated by a stem cell normally located at the base of the intestinal crypt." To our knowledge, no experiments have been reported that critically address any of these four mechanisms.

It is generally accepted that a germ-line *APC* mutation leads to the proliferative shift in FAP crypts because: (*a*) all cells in the crypt carry the germ-line mutation; (*b*) the $APC^{Min/+}$ mouse, which also carries a germ-line *APC* mutation, similarly displays proliferative crypt changes in histologically normal intestinal mucosa (11); and (*c*) humans who have a different CRC-predisposing germ-line mutation that is responsible for hereditary nonpolyposis CRC do not show a proliferative shift in histologically normal colonic crypts (12). Nonetheless, the mechanism that defines the connection between any or all of the known molecular functions of APC (13) that would be lost because of *APC* mutation and the proliferative shift as seen in FAP patients has not been established.

Model Design and Computer Simulation. To investigate the cellular mechanism responsible for the proliferative shift in FAP crypts, which would increase our understanding of CRC initiation, we created a CPD model.

The CPD model (Fig. 1) was designed to simulate the cellular dynamics of the colonic crypt (14, 15). The model takes into account that: (*a*) cell proliferation, differentiation, and apoptosis occur continuously in the crypt; (*b*) as epithelial cells migrate up the crypt column, they change in their capacity for cell division and differentiation; and (*c*) the crypt, even in FAP patients, represents a highly regulated steady-state system whereby a constant number of cells is maintained via a balance between cell generation in the lower part of the crypt and cell loss at the top of the crypt.

Eight cell types (STs; cells in different phases of the cell cycle; and Ds, TDs, and ACs) were included in the model, and a rate equation was written that expresses the rate of change of the population size for each cell type as a function of time (Fig. 1). The CPD model also included expressions for feedback loop mechanisms. Selection of the first set of rate constant values was, by necessity, arbitrary because rate constant values for steps shown in Fig. 1 have not yet been reported. The number of STs in murine intestinal crypts has been reported to be 4–16 STs/crypt (14). Thus, an ST^0 of 10 was chosen.

Rate equation sets were solved by numerical integration with Mathematica equation-solving software (Wolfram Research, Inc., Champaign, IL). CPD model output was graphically displayed as the percentage of S-phase cell

Received 9/4/01; accepted 10/19/01.

The costs of publication of this article were defrayed in part by the payment of page charges. This article must therefore be hereby marked *advertisement* in accordance with 18 U.S.C. Section 1734 solely to indicate this fact.

[1] Supported by CA*TX, Inc., the Cancer Fund (Omaha, NE), and Grants NIH R21 CA71531-02 and NIH R15 AR41530-01.

[2] To whom requests for reprints should be addressed, at Thomas Jefferson University, Medical Office Building, Suite 400, 1100 Walnut Street, Philadelphia, PA 19107. Phone: (215) 955-6648; Fax: (215) 503-2983; E-mail: Bruce.Boman@mail.tju.edu.

[3] Present address: Center for Healthy Aging, Saint Joseph Medical Center, Chicago, IL 60657.

[4] Present address: ValiGen SA, 92086 Paris-La-Defense, France.

[5] The abbreviations used are: CRC, colorectal cancer; FAP, familial adenomatous polyposis; LI, labeling index; CPD, cellular proliferation/differentiation; *APC*, adenomatous polyposis coli gene; D, nonterminally differentiated cell; TD, terminally differentiated cell; ST, stem cell; ST^0, initial number of STs; AC, apoptotic cell.

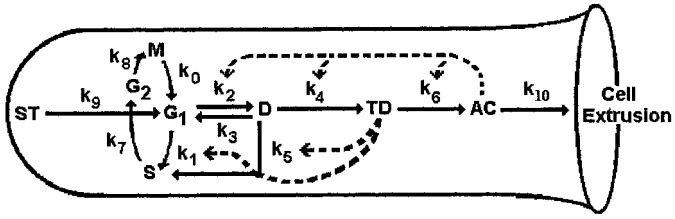

Fig. 1. CPD model design. This scheme from which the computer model was constructed can be viewed as having two parts within the main mechanism (*solid arrows*). Cellular proliferation (*left-hand side* of scheme) is a closed system specified by the cell cycle ($G_1 \rightarrow S \rightarrow G_2 \rightarrow M \rightarrow G_1 \rightarrow_{...}$) and is the "default" mechanism for generating cells within the system. Cellular differentiation and apoptosis (*right-hand side* of scheme) represents an open system in which cells exit the cell cycle by the differentiation/apoptosis pathway ($G_1 \rightarrow D \rightarrow TD \rightarrow AC$). Ds and TDs represent the population of all differentiated cell types found in human crypts. The scheme also shows STs as the initial cell type for generation of G_1 phase cells ($ST \rightarrow G_1$), which simulates the biological mechanism by which STs at the crypt base generate progeny cells for crypt cell renewal. STs and the differentiation pathways are coupled to the cell cycle at the G_1 phase. Also incorporated are pathways for dedifferentiation of Ds ($D \rightarrow G_1$) and proliferation of Ds ($D \rightarrow S$). Cell loss is depicted by exit of ACs from the system, which simulates biological extrusion or phagocytosis of ACs at the crypt top.

Rate constants for each step in the model and rate equations for the rate of change of each cell type population are as follows:

$$dM/dt = k_8[G_2] - k_0[M]$$

$$dST/dt = -k_9[ST]$$

$$dG_1/dt = k_9[ST] + 2\,k_0[M] + k_3[D] - k_1[G_1]/(1 + [TD]) - k_2[G_1](1 + [AC]^2)$$

$$dD/dt = k_2[G_1]\,(1 + [AC]^2) - k_3[D] - k_4[D]\,(1 + [AC]^2) - k_5[D]/(1 + [TD])$$

$$dTD/dt = k_4[D]\,(1 + [AC]^2) - k_6[TD](1 + [AC]^2)$$

$$dS/dt = k_1[G_1]/(1 + [TD]) + k_5[D]/(1 + [TD]) - k_7[S]$$

$$dG_2//dt = k_7[S] - k_8[G_2]$$

$$dAC/dt = k_6[TD]\,(1 + [AC]^2) - k_{10}[AC]$$

The CPD model design also includes two feedback loop mechanisms (*dashed arrows*). In the negative feedback mechanism, the TD cell population regulates two steps, $D \rightarrow S$ and $G_1 \rightarrow S$, whereby rate constants k_1 and k_5 are controlled by the expression $(1/(1 + [TD]))$. In the positive feedback mechanism, the AC population regulates three steps, $G_1 \rightarrow D$, $D \rightarrow TD$, and $TD \rightarrow AC$, whereby rate constants k_2, k_4, and k_6 are controlled by the expression $(1 + [AC]^2)$. Adjustable parameter values in the model included ST^0 and the 11 rate constants that govern the rate of the various cell cycle and differentiation/apoptosis steps. Rate constants represent inverse relative time units.

population (*Y axis*) as a function of cell crypt axis position (*X axis*). Goodness-of-fit with the biological data were calculated using nonlinear regression analysis to yield R^2 (GraphPad Software, Inc., San Diego, CA).

Results

Computer simulation of the control LI biological data (Fig. 2*A*) from healthy unaffected individuals was accomplished by systematically adjusting parameter values (rate constants and ST^0) and modifying the model design (*e.g.*, adding feedback loops). Using this iterative approach, a set of parameter values and a model design (Fig. 1) were achieved that generated output that fit with control LI data (Fig. 2*B*). "Goodness-of-fit" analysis showed an outstanding fit of simulation data to control biological data ($R^2 = 0.98$).

To test the four mechanisms (discussed above in "Materials and Methods") for the proliferative shift in FAP crypts, it was determined whether perturbation of any single CPD model parameter gave an S-phase curve that mimics this LI shift. When rate constant values that had fit best with the control LI were individually increased or decreased, none of the resultant S-phase profiles fit the FAP biological data (Fig. 3). Perturbations of k_0, k_3, k_6, k_8, k_9, and k_{10} had virtually no effect on the S-phase cell profile (but did affect other cell type profiles; data not shown). Perturbations of k_1, k_2, k_4, k_5, and k_7 caused either an increase or decrease in the peak height of the S-phase curve and slight shifts in peak position along the crypt axis (Fig. 3). However, none of these rate constant perturbations yielded curves that mimicked the LI shift in FAP. Modifying the feedback loops also failed to simulate FAP LI data.

In contrast, when ST^0 was perturbed, the S-phase curve showed major shifts along the crypt axis. Fig. 4*A* shows that a right shift occurs when ST^0 is increased from 10 to 15, which mimics the proliferative shift from control to FAP crypts (Fig. 2*A*).

"Goodness-of-fit" analysis was used to quantitatively determine which values for initial number of STs yielded model data output that best fit with the biological data. This analysis resulted in bell-shaped curves, the peaks of which indicated best fits with either control or FAP data (Fig. 4*B*). An ST^0 of 11 yielded an S-phase curve that best fit the control LI ($R^2 = 0.98$), whereas an ST^0 of 16 yielded an S-phase curve that best fit the FAP LI ($R^2 = 0.90$). Higher and lower values of ST^0 yielded S-phase curves that had poorer goodness-of-fit values for FAP and control. The effect of this perturbation in ST^0 (from 11 to 16) in the model suggests that an increase of ~50% in the number of STs in the crypt underlies the shift observed biologically from control to FAP LI (see Fig. 4*C*).

Discussion

Although other models have been developed to study intestinal crypt cellular dynamics (14), to our knowledge our CPD model is the first designed to investigate the cellular etiology of the proliferative abnormality in normal-appearing (nonaberrant) FAP crypts.

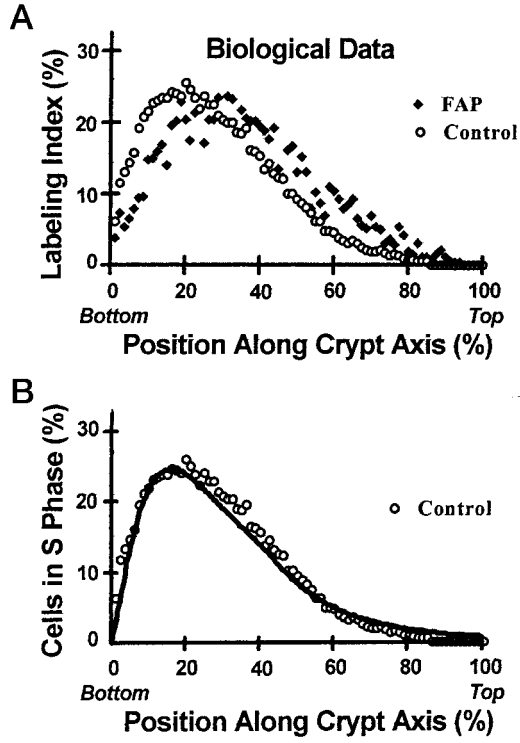

Fig. 2. *A*, the biological data from FAP and control crypts. The biological data modified from those of Potten *et al.* (5) are displayed as the percentage of bromodeoxyuridine-labeled cells as a function of cell position along the crypt axis for both healthy unaffected human controls (○) and FAP patients (◆). Comparison of the FAP LI to control LI shows that the FAP proliferative abnormality (resulting from a germ-line *APC* mutation) involves a shift in the LI toward the crypt top. Specifically, the FAP LI as compared with the control LI shows a shift in the S-phase curve peak position from 20 to 31.25% along the crypt axis, whereas a slight decrease was observed in the peak height from 25.58% to 23.65% S-phase cells. This proliferative abnormality does not appear to involve hyperproliferation because the total number of labeled cells in FAP crypts is not significantly increased (*i.e.*, the FAP:control ratio for "area-under-the-curve" is 1.05). *B*, "best-fit" simulation of control biological data. Results on "best-fit" CPD model simulation of the control LI are displayed (———) as the percent of S-phase cells (*Y axis*) *versus* cell crypt axis position (*X axis*). Rate constant values (k_0 to k_{10}) that gave the best fit for control biological data were, respectively, 0.05, 0.03, 0.025, 0.00625, 0.025, 0.025, 0.018, 0.0325, 0.025, 0.125, and 0.

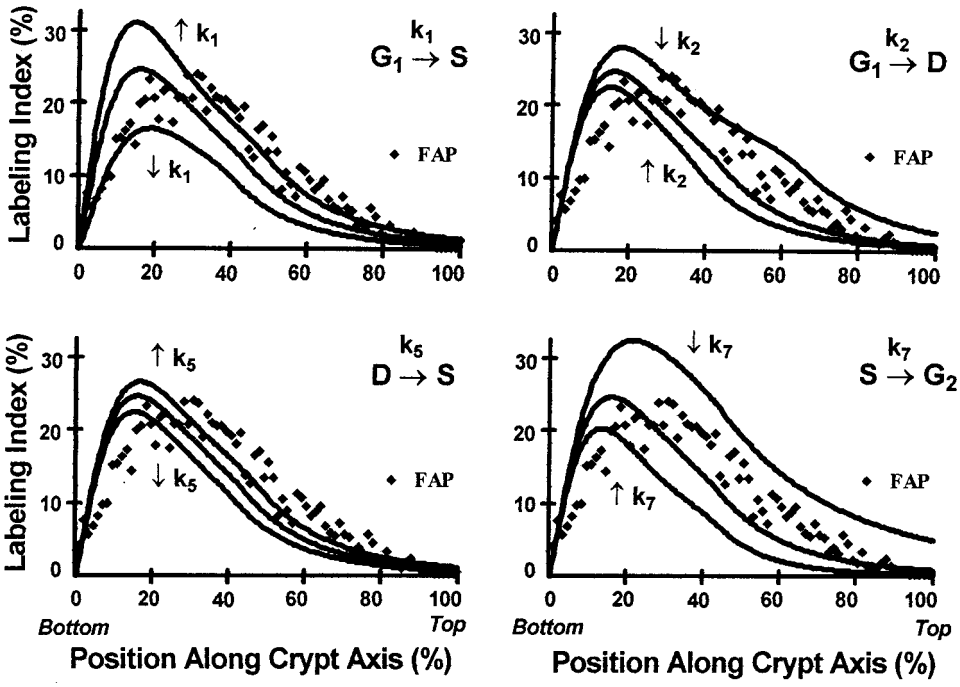

Fig. 3. Attempts to simulate the FAP biological data by perturbation of rate constant values. The "best-fit" CPD model output for the control LI is the *middle curve* in each panel. The S-phase profiles (*upper* and *lower curves*) resulting from perturbation of the rate constants k_1, k_2, k_5, and k_7 are also shown after a 50% increase or decrease in each parameter value. Perturbation of k_4 gave graphical output (not shown) that was nearly identical to results shown for perturbation of k_2. These results show that perturbation of rate constants k_1, k_2, k_4, k_5, and k_7 failed to produce a S-phase curve profile that fits the FAP biological data. Perturbation of k_0, k_3, k_6, k_8, k_9, and k_{10} had no appreciable effect on the S-phase profile (but did affect other cell type profiles; data not shown).

Our study shows that theoretical interpretation of complex biological processes based on mathematical modeling has several advantages. For instance, our modeling of the dynamics of crypt cell renewal provided a defined and quantitative context in which different outcomes could be evaluated and compared following changes in input parameters. In addition, modeling was used to quantitatively test the validity of mechanisms posed previously to explain the cellular etiology of the proliferative shift in FAP. Finally, modeling provided a rapid and practical method to conduct "experiments" that have not, because of system complexity, been accomplished previously.

Our simulation results provide insight into the origin of the proliferative abnormality in FAP:

(*a*) The fact that a single mechanistic design (Fig. 1) was able to afford our simulation of biological data from both control and FAP subjects suggests that the FAP proliferative abnormality *in vivo* does not require an additional or new biological mechanism that alters crypt epithelial cell renewal.

(*b*) The fact that an identical set of rate constant values gave the best fit with both control and FAP biological data (Figs. 2*B* and 4*C*) suggests that the FAP proliferative abnormality is not attributable to a cellular mechanism that alters the rate of cell cycle proliferation, differentiation, and/or apoptosis of non-STs.

(*c*) Modeling suggests that an expansion in the crypt ST population is sufficient to explain the observed proliferative abnormality in FAP.

Because we modeled the crypt proliferative abnormality found in histologically normal crypts of FAP patients, who are individuals known to carry a germ-line *APC* mutation, it seems conceivable that crypt ST overproduction is caused by a mutation in *APC*. In FAP patients, the colonic STs will all contain the germ-line *APC* mutation, and it is this mutant ST population that is expanded according to our modeling. Thus, there may be an APC-based mechanism by which mutant STs increase in number. Extrapolation of this line of reasoning suggests that if an *APC* mutation occurs in a single colonic ST because of an acquired genetic change, it might give rise to a mutant ST population that expands in the colonic crypt. If that proves to be the case, it would provide a key mechanism at the cellular level that links the initiating events at the genetic level and at the tissue level in CRC tumorigenesis. Because the initiating genetic event in sporadic CRC is thought to involve an acquired *APC* mutation (13), initiation of this common form of CRC may also involve crypt ST overproduction. Because STs are thought to be the cell of origin in many types of solid and hematological malignancies, this model of CRC initiation via ST overproduction may be generally relevant.

CPD modeling suggests a corollary hypothesis, *i.e.*, that APC-based molecular mechanisms in the colonic crypt might normally function to control the number of colonic STs. Although such a regulatory property of APC has not yet been described, indirect biological evidence is consistent with this hypothesis. In the homozygous mutant Tcf4 mouse, inactivation of the Tcf4 transcription factor (mimicking the downstream molecular effect of APC) leads to depletion of epithelial ST populations in the small intestine (16). These results coupled with the fact that activation of Tcf4 is known to occur when *APC* is mutant support the hypothesis that APC-linked molecular processes control ST number. On the basis of these observations, it would be predicted that the ST population is expanded in FAP crypts because a germ-line *APC* mutation would lead to activation of Tcf4. This prediction is consistent with our evidence from CPD modeling indicating that expansion of the ST population occurs in the FAP crypt.

If *APC* mutation leads to an increased number of crypt STs, it seems logical to speculate that when the remaining wild-type *APC* allele is lost (*i.e.*, the "second hit"), a further increase in the number of STs will probably occur. This second hit in *APC* usually occurs by the adenomatous polyp stage (2) in humans and $APC^{Min/+}$ mice. Moreover, mutation of both *APC* alleles is "sufficient" for the growth of early colorectal adenomas in FAP patients (17). Therefore, further clonal expansion of the ST population attributable to a second hit in *APC* could conceivably contribute to adenoma development. Indeed, CPD modeling shows that increasing the initial number of STs beyond 16 causes an even greater shift in the S-phase profile toward the crypt top (Fig. 4*A*). Others have proposed mechanisms to explain how the earliest identifiable morphological change (*i.e.*, aberrant crypt foci) in colon carcinogenesis develops and progresses toward adenomas (18). In contrast, our "ST overproduction" mechanism attempts to explain events that precede the appearance of any morphological changes. Hence, this "ST overproduction mechanism" might help understand the processes involved in the transition to early morphological changes. Because adenomas accumulate mutations

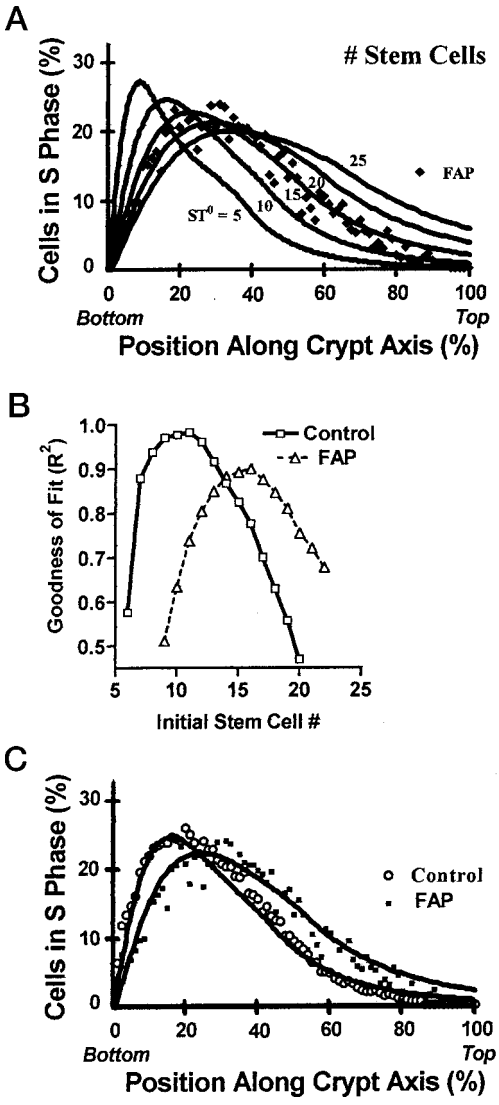

Fig. 4. *A*, computer output showing that the S-phase curve shifts along the crypt axis attributable to increasing ST^0. Perturbations of other model parameters failed to produce such a right-shift of the S-phase curve. Numbers next to the curves indicate values for ST^0. *B*, goodness-of-fit of CPD model output with control and FAP biological data. Goodness-of-fit of simulation data to LI biological data were calculated using nonlinear regression analysis based on a polynomial curve derived from the simulated S-phase curve output. The polynomial curve was then used to determine fit with the biological data. Specifically, regression analysis was accomplished by generating a seventh order polynomial for the simulated S-phase cell population/crypt axis data and then by comparing the polynomial with biological LI data to yield R^2s. R^2 is the fraction of the variation that is shared between *X* and *Y*, which ranges between 0 and 1.0 with 0 being an absence of fit and 1.0 being an exact fit. *C*, "best-fit" simulation of FAP and control biological data. The figure shows "best-fit" CPD model simulation (*solid black lines*) in relation to the control and FAP biological data (*data points*). Rate constant values (k_0 to k_{10}) that gave the best-fit for FAP biological data were the same as those values for best-fit of control biological data (see Fig. 2*B*).

in other genes, the possibility that other mechanisms, such as aberrant colonocyte maturation, contribute to adenoma formation must also be considered.

Our "ST overproduction" hypothesis is also consistent with the ST model of tumor growth based on the concept of hierarchical proliferation (19). The hierarchical concept holds that neoplasms have a cell-renewal hierarchy that is similar to normal tissues, and tumors contain three types of cells: (*a*) proliferating, self-renewing tumor stem cells; (*b*) proliferating, nonrenewing transitional cells; and (*c*) nonproliferating, differentiated end cells. The hierarchical concept also proposes that although the ST component of tumors is a small subset within the total tumor cell population, its expansion is the basis of growth of tumors.

That cancer originates from STs is not a new concept (20), particularly in relation to the origin of leukemias and of teratomas. Indirect evidence also supports a ST origin for solid tumors such as CRC. It is reasoned that because tumorigenesis in the colon is a relatively slow process, short-lived non-ST populations within crypts are considered an unlikely origin of CRC (9). Additionally, histological evidence from adenomas in $APC^{Min/+}$ mice (10) and human colon cancers (20) indicates that multiple types of differentiated intestinal cells exist in these tumors, which suggests that they arise from a multipotent crypt ST. The present study now provides a mechanism for how crypt STs might be involved in the origin of CRC.

In conclusion, CPD modeling provides insights into the "enormous complexities" of tumorigenesis (1) and has provided a theoretical foundation for understanding CRC initiation and adenoma development. On the basis of this view of tumorigenesis, effective CRC therapy and chemoprevention will require elimination or control of mutant ST populations.

Acknowledgments

We thank Catherine Boman (President, CA*TX, Inc.) for invaluable administrative assistance, Drs. Steve McKenzie and Scott Waldman for reviewing the manuscript, and Drs. Alfred Knudson and Saul Surrey for suggestions.

References

1. Sonnenschein, C., and Soto, A. M. The enormous complexity of cancer. *In:* The Society of Cells—Cancer and Control of Cell Proliferation, pp. 99–109. New York: BIOS Scientific Publishers Ltd. and Springer-Verlag, 1999.
2. Levy, D. B., Smith, K. J., Beazer-Barclay, Y., Hamilton, S. R. Vogelstein, B., and Kinzler, K. W. Inactivation of both APC alleles in human and mouse tumors. Cancer Res., *54:* 5953–5958, 1994.
3. Deschner, E. E., Lewis, C. M., and Lipkin, M. *In vitro* study of human rectal epithelial cells: atypical zone of [H^3]thymidine incorporation in mucosa of multiple polyposis. J. Clin. Investig., *42:* 1922–1928, 1963.
4. Cole, J. W., and McKalen, A. Studies on the morphogenesis of adenomatous polyps in the human colon. Cancer (Phila.), *16:* 998–1002, 1963.
5. Potten, C. S., Kellett, M., Rew, D. A., and Roberts, S. A. Proliferation in human gastrointestinal epithelium using bromodeoxyuridine *in vivo*: data for different sites, proximity to a tumor, and polyposis. Gut, *33:* 524–529, 1992.
6. Deschner, E. E., and Lipkin, M. Proliferative patterns in colonic mucosa in familial polyposis. Cancer (Phila.), *35:* 413–418, 1975.
7. Biasco, G., Paganelli, M. P., Miglioli, M., and Barbara, L. Cell proliferation biomarkers in the gastrointestinal tract. J. Cell Biochem. Suppl., *16G:* 73–78, 1992.
8. Lipkin, M. Phase 1 and Phase 2 proliferative lesions of colonic epithelial cells in diseases leading to colonic cancer. Cancer (Phila.), *34* (Suppl.)*:* 878–888, 1974.
9. Potter, J. D. Colorectal cancer: molecules and populations. J. Natl. Cancer Inst., *91:* 916–932, 1999.
10. Moser, A. R., Dove, W. F., Roth, K. A., and Gordon, J. I. The Min (Multiple Intestinal Neoplasia) mutation: its effect on gut epithelial cell differentiation and interaction with a modifier system. J. Cell Biol., *116:* 1517–1526, 1992.
11. Mahmoud, N. N., Boolbol, S. K., Bilinski, R. T., Martucci, C., Chadburn, A., and Bertagnolli, M. M. *Apc* gene mutation is associated with a dominant-negative effect upon intestinal cell migration. Cancer Res., *57:* 5045–5050, 1997.
12. Green, S. E., Chapman, P., Burn, J., Bennett, M., Appleton, D. R., Varma, J. S., and Mathers, J. C. Colonic epithelial cell proliferation in hereditary non-polyposis colorectal cancer. Gut, *43:* 85–92, 1998.
13. van Es, J. H., Giles, R. H., and Clevers, H. C. The many faces of the tumor suppressor gene *APC*. Exp. Cell Res., *264:* 126–134, 2001.
14. Potten, C. S., and Loeffler, M. Stem cells: attributes, cycles, spirals, pitfalls and uncertainties. Lessons from the crypt. Development (Camb.), *110:* 1001–1020, 1990.
15. Bedi, A., Pasricha, P. J., Akhtar, A. J., Barber, J. P., Bedi, G. C., Giardiello, F. M., Zehnbauer, B. A., Hamilton, S. R., and Jones, R. J. Inhibition of apoptosis during development of colorectal cancer. Cancer Res., *55:* 1811–1816, 1995.
16. Korinek, V., Barker, N., Moerer, P., Van Donselaar, E., Huls, G., Peters, P. J., and Clevers, H. Depletion of epithelial stem-cell compartments in the small intestine of mice lacking Tcf-4. Nat. Genet., *19:* 379–383, 1998.
17. Lamlum, H., Papadopoulou, A., Ilyas, M., Rowan, A., Gillet, A., Hanby, A., Talbot, I., Bodmer, W., and Tomlinson, I. APC mutations are sufficient for the growth of early colorectal carcinomas. Proc. Natl. Acad. Sci. USA, *97:* 2225–2228, 2000.
18. Roncucci, L., Pedroni, M., Vaccina, F., Benatti, P., Marzona, L., and De Pol, A. Aberrant crypt foci in colorectal carcinogenesis: cell and crypt dynamics. Cell Prolif., *33:* 1–18, 2000.
19. Kummermehr, J., and Trott, K. R. Tumour stem cells. *In:* C. S. Potten (ed.), Stem Cells, pp. 363–399. London: Academic Press, 1997.
20. Pierce, G. B., Shikes, R., and Fink, L. M. Origin of neoplastic stem cells. *In:* Cancer—A Problem in Developmental Biology, pp. 68–87. New York: Prentice Hall, 1974.

Computer Modeling Implicates Stem Cell Overproduction in Colon Cancer Initiation

Bruce M. Boman, Jeremy Z. Fields, Oliver Bonham-Carter, et al.

Cancer Res 2001;61:8408-8411.